View metadata, citation and similar papers at core.ac.uk

brought to you by CORE

provided by DSpace@MIT

Investigation of the Dimensional Variation of Microstructures Through the μMIM Process

FU G. [3], READING I.[1], LI S.G.[1], CHATURVEDI P.[1], TOR, S.B. [3], YOON S.F. [2] , FANG Z.P. [1]
and YOUCEF-TOUMI K.[4]
[1] Precision Measurements Group, SIMTech
[2] School of Electrical and Electronic Engineering, NTU
[3] School of Mechanical and Aerospace Engineering, NTU
[4] Dept. of Mechanical Engineering, MIT

INTRODUCTION

The mass production of components with dimensions in the micron and sub-micron range is anticipated to be one of the leading technology areas for the present century and to be of high market potential [1]. Micro metal injection molding (μMIM) has the potential to be an important contributor to this industry as it can produce precise metallic microstructures in large quantities at a relatively low production cost. The μMIM process is a miniaturization of metal injection molding (MIM) methods. The process comprises of four main steps: mixing, injection molding, debinding and sintering as shown in Fig.1 [2]. A metallic powder is mixed with a binder system to form the feedstock. The feedstock is then injection molded into the required shape and the binder removed via thermal or other means. The final microstructures are obtained by sintering the remaining powder in a controlled environment. In this work, the dimensional variation of the microstructures, in particular the warpage, roughness and volume variation, at each stage of the μMIM process was quantified and compared. The results of a preliminary study of the sensitivity of warpage of the microstructures to the packing pressure are also reported.

SAMPLE PREPARATION

The experimental test pattern consisted of a part with an array of 24 x 24 pillars. Each pillar's design dimensions are a diameter of Φ100μm, a height of 200μm and a pitch of 200μm.

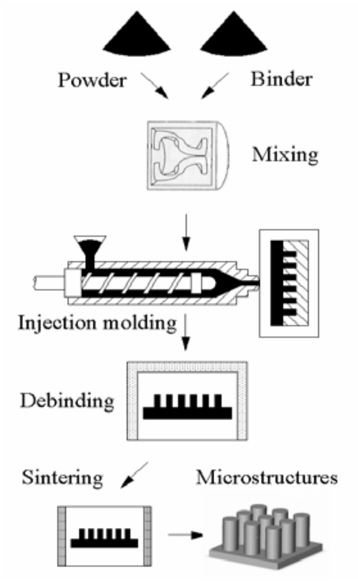

Fig. 1: The processing steps of μMIM

316L stainless steel feedstock with polyacetal-based binder system was used. This powder has a particle size of D_{50} = 4 μm. To replicate the microstructures, a 5 mm × 5 mm × 0.5 mm silicon master with 24 × 24 (576) microcavities was used. The microcavities are produced using deep reactive ion etching (DRIE). In the injection molding step, a round disc of ϕ16 mm and thickness 1.5 mm with an array of ϕ100 μm microstructures at the center is injection molded. In this step, one of the important parameters is the packing pressure that ensures the addition of fresh melt into the mold cavity to compensate for the effects of thermal contraction of the melt during cooling.

After the injection molding step, the molded part with microstructures was debound catalytically in a Kendro VT6060 MU-2 air circulation drying oven. Polyacetal has the favorable property of depolymerizing catalytically under acidic conditions yielding formaldehyde. The oven is a steel-lined gas-tight furnace, which is equipped with a fan to achieve thorough mixing and proper heat transfer. The oven is heated and flushed with nitrogen of 2 bar to avoid an explosive atmosphere during debinding, at the same time avoiding excessive surface oxidation of sensitive powders. The flow rate of nitrogen is set as 500 l/h. After reaching the process temperature of 120 °C, the catalyst (100 % nitric acid) is metered into the hot purge gas. The concentration of the gaseous nitric acid ranges from 0.1 to 5 vol.%, depending on the material and the loading of the oven. In this study, the acid rate was set as 35 ml/h. The exhausted gas, mainly formaldehyde in the nitrogen carrier gas is burnt with excess air.

Sintering is conducted in a reduced gas environment. First, the debound part is heated from room temperature to 600 °C at a heating rate of 7 °C/h, then held for one hour at 600 °C. The part is then heated from 600 °C to the sintering temperature 1300 °C at a heating rate of 7 °C/h and held for one hour. After that, the sintered part is naturally cooled in the furnace down to room temperature. Fig.2 shows local SEM images of molded, debound and sintered part with ϕ100 µm microstructures.

These micro-pillars like microstructures produced as test structures also represent the needs of potential applications using mold inserts for micro plastic injection molding, e.g. microtiter-plates for DNA test [3], biomedical devices (nerve stimulation needles) [4], microfluidic devices [5].

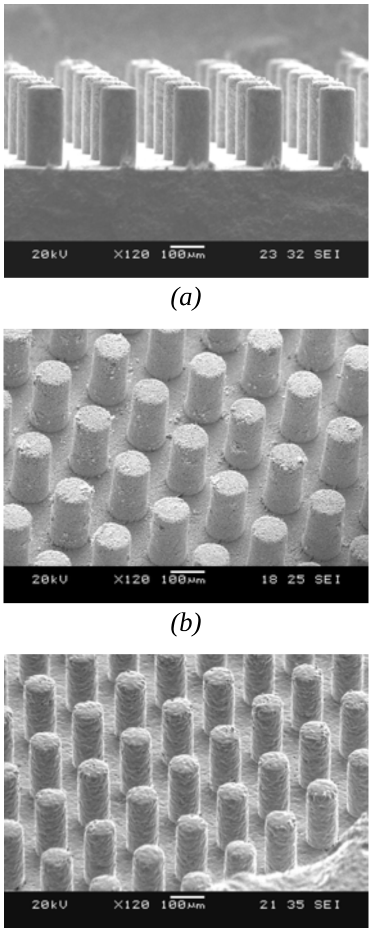
20kV X120 100µm 23 32 SEI
20kV X120 100µm 18 25 SEI
20kV X120 100µm 21 35 SEI

(a)

(b)

(c)

Fig.2: SEM images of section of pillar array for (a) molded,(b) debound and (c) sintered parts

SAMPLE CHARACTERISATION

A very important aspect in µMIM is the characterization of the dimensional variation of the microstructures at the different process steps. As the three main processes of injection molding, debinding and sintering take place in a high pressure and high temperature environment, it may easily result in significant variation in three key parameters namely global warpage of the microstructures, surface roughness and local pillar volume. Variability may arise due to the use of inappropriate processing parameters such as packing pressure in the injection molding step or heating rate in the sintering step . Of the three parameters, the global warpage of the final product is the most important and must be guaranteed to be below a minimum level as it impacts not only the final geometric dimensions but also the mechanical properties.

In this paper, the material and dimensional variation of the microstructures throughout each step of the µMIM process were quantified and compared using a Veeco interferometer (Model: NT 3300). Global warpage, roughness and dimensional shrinkage data was extracted. A preliminary study of the variation due to the effect of packing pressure on these parameters of the microstructures was also conducted.

Figure3 shows the a 3D representation of the global profile of a typical sintered part - with the pillar array protruding upwards from the base. By extracting a cross-section through the central point of the profile in Fig.3 (avoiding the pillar regions), the radius of curvature and roughness of the substrate was be examined.

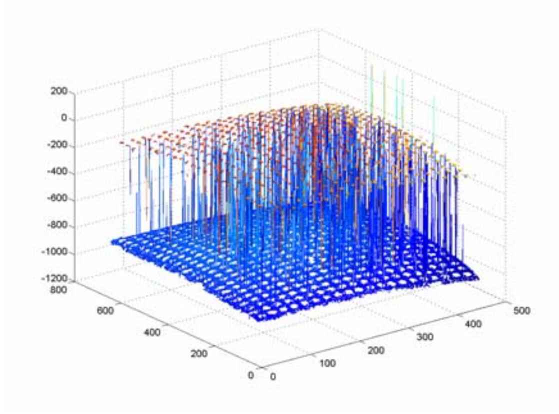

Fig.3: Typical 3D profile of a sintered part

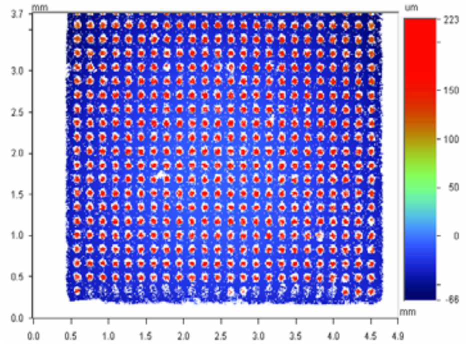

Fig.4: Plan view of a sintered part profile

The plan view indicates that even at this low magnification good quality data could be obtained from most of the pillars. The white regions around each pillar are regions where no data was recovered due to the near-vertical sidewalls.

MEASUREMENT RESULTS

The warpage of the base profile is presented below. As the part is symmetrical in the x and y axes just the results in the x direction are illustrated and analyzed in what follows. Profiles in the y direction were observed to exhibit similar behaviour.

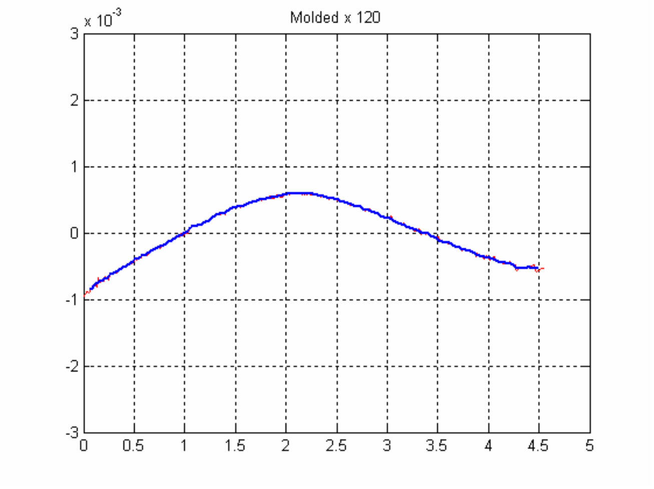

(a)

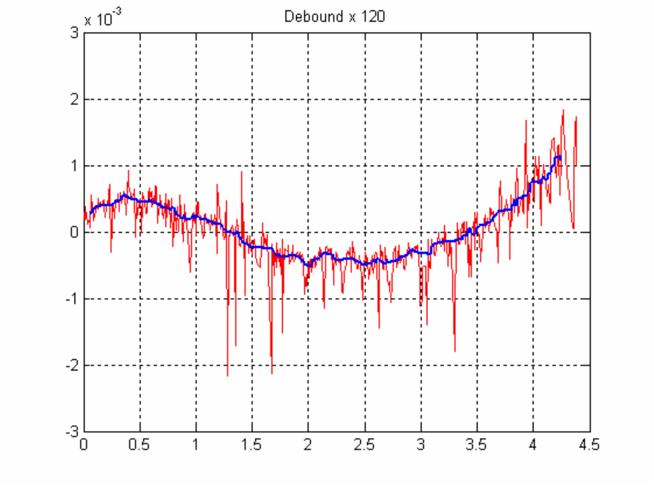

(b)

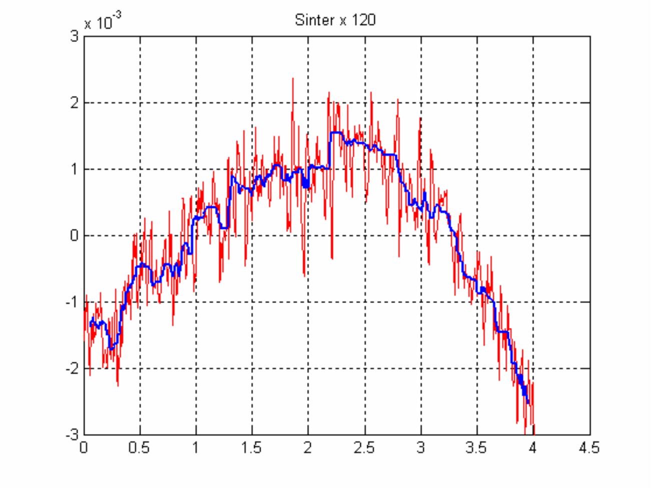

(c)

Fig.5: Preprocessing of data for (a) molded,(b) debound and (c) sintered parts formed at 120 bar

Figure 5 shows the results of pre-processing applied to the raw data to allow clear comparison of overall warpage. This was necessary as the original data for the debound and sintered is broken and noisy due to the porous surface. In the figure the strong line represents the median calculated over 20 neighbouring points. It is overlaid onto a lighter line showing the original raw data. From this point on further graphs all show pre-processed data.

Fig.6 shows the variation of warpage from the Silicon mold as the piece progresses through the forming stages.

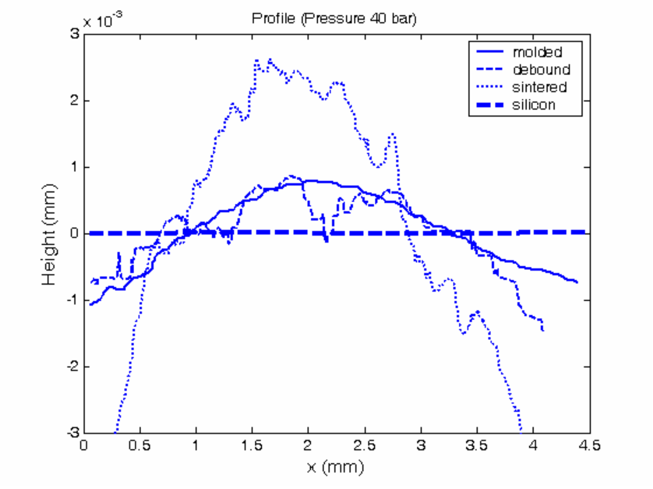

(a)

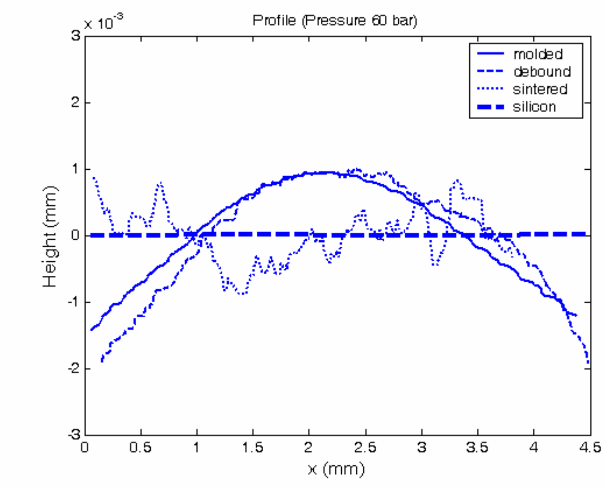

(b)

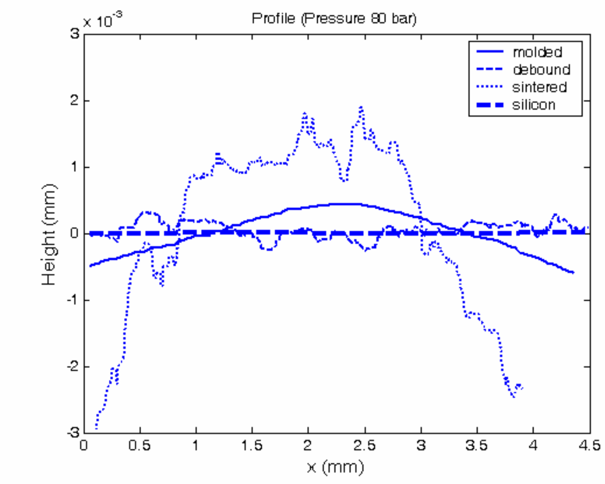

(c)

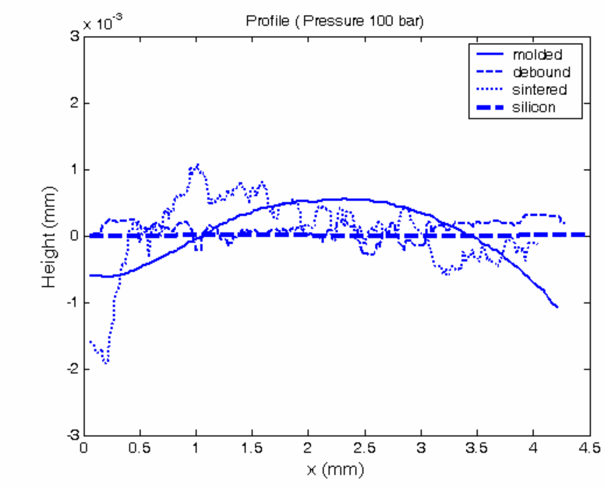

(d)

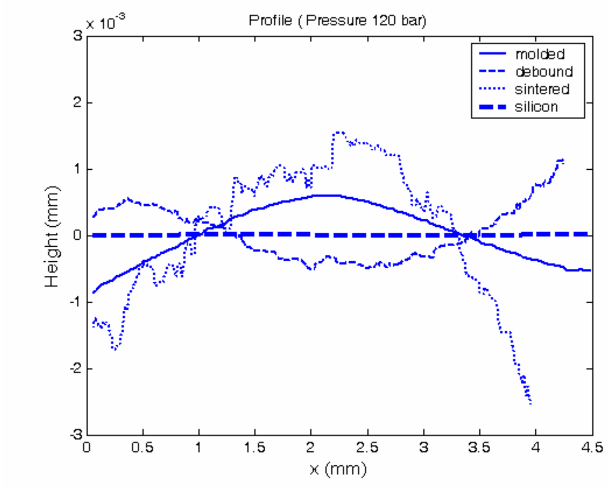

(e)

Fig.6: Variation in profile by each forming stage at (a)40bar,(b)60bar,(c)80bar,(d)100bar,(e)120bar

Interestingly the curvatures for the molded parts were found to be always positive (defining centre raised as positive). The positive curvature is believed to result from residual stress and deformation due to sliding friction between the microstructures and the microcavities of the silicon master during demolding (the ejection of the molded part out of the silicon master). The debinding process can be seen to cause a flattening of this curvature to cancel (80bar) or even negate (120bar) the initial curvature. It is further observed that after sintering there is a tendency for the profile to return to the original positive curvature. This is believed to be due to the release of residual stress in the molded parts when the temperature is increased and the binder system is decomposed in the debinding step. The magnitude of the curvature of the sintered parts was found to be larger than at any other process stage.

This pattern is reinforced by Figure 7 which presents the profile grouped by forming stage. The consistent positive curvature at the molded stage is particularly apparent.

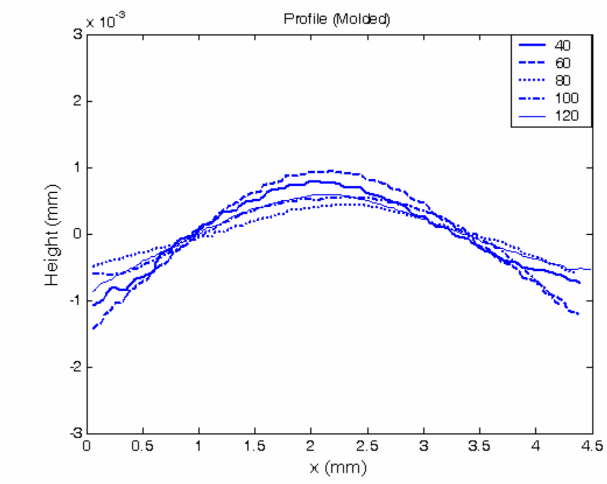

(a)

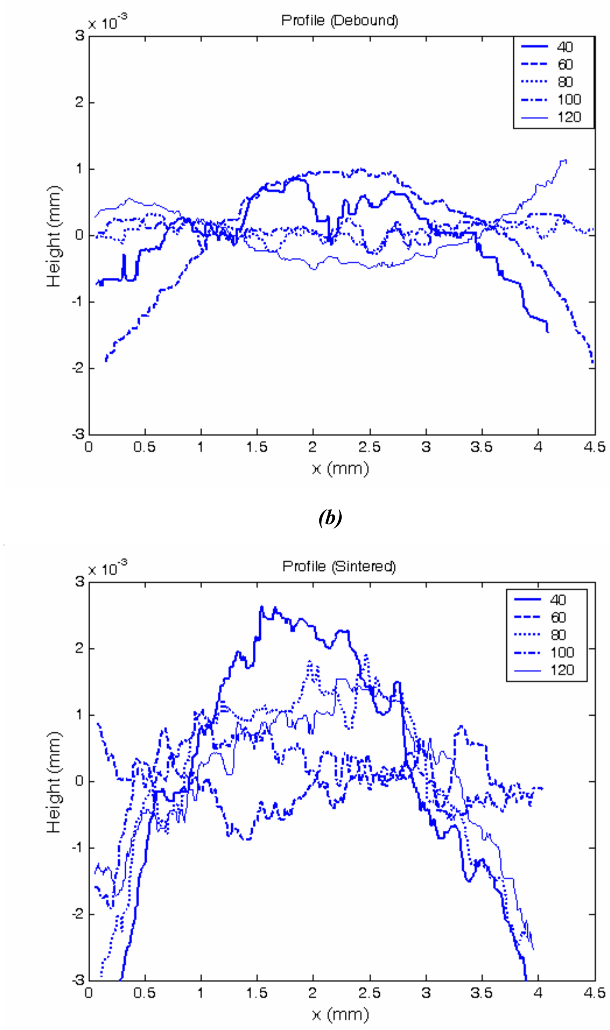

(b)

(c)

Fig.7: Variation in profile at each forming stage (a)molded,(b)debound,(c)sintered

Given the approximately unimodal nature of the profiles a LMS circle fitting approach was used to estimate the radius of curvature for each data sets. This allows these patterns to be presented in a compact form, Figure 8. Interestingly it indicates a pressure sensitive effect as it can be seen how the flattening effect between the molded and debound stages is less at 40 & 60 bar than at the higher pressures. Despite this after sintering all cases recover to within a similar curvature range.

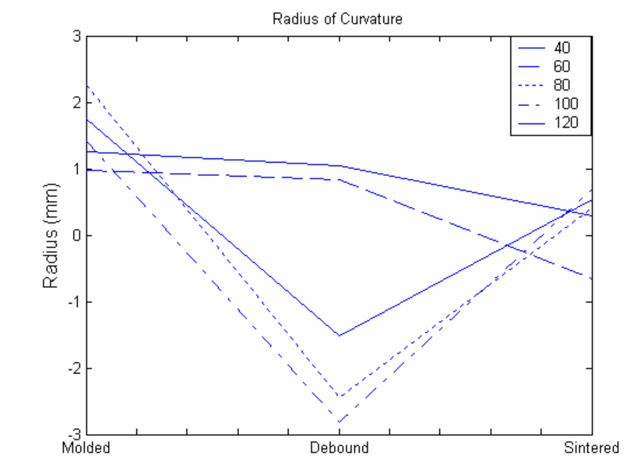

Fig.8: Curvature by process stage for a range of molding pressures

By mathematically removing the overall curvature from each data set, an estimate of the mean root square roughness (Rq) for each curve was obtained. Figure 9 shows the roughness for the parts at different process stages over the range of packing pressures. For the molded parts, there was little roughness variation compared with the master. As the polymer was burned away in the debinding and the sintering steps, the roughness predictably increases. According to these results it is interesting to note that there is no evident correlation between the packing pressure used in the injection molding step and the surface roughness of the final part and microstructures.

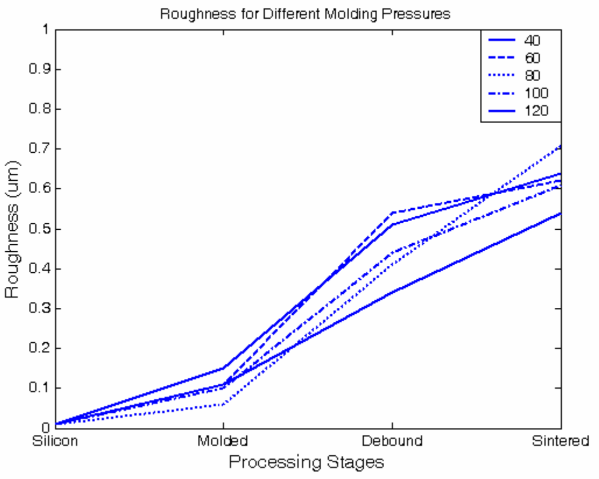

Fig.9: Roughness by process stage for a range of molding pressures

Dimensional shrinkage was assessed by measurement of the height and diameter of four central pillars from each sample. These were measured in the interferometer at high magnification to obtain more complete data due to the high numerical aperture. Typical data quality is indicated by the single pillar profile given in Figure 10.

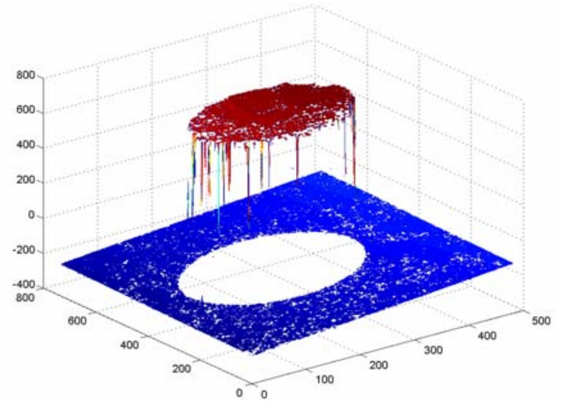

Fig.10: High magnification profile of a single pillar for dimensional shrinkage study

The mean diameter and height of the microstructures was estimated from these measurements and the results are shown in Figure 11. It can be seen that the diameters of the microstructures expand by a few percent after debinding.

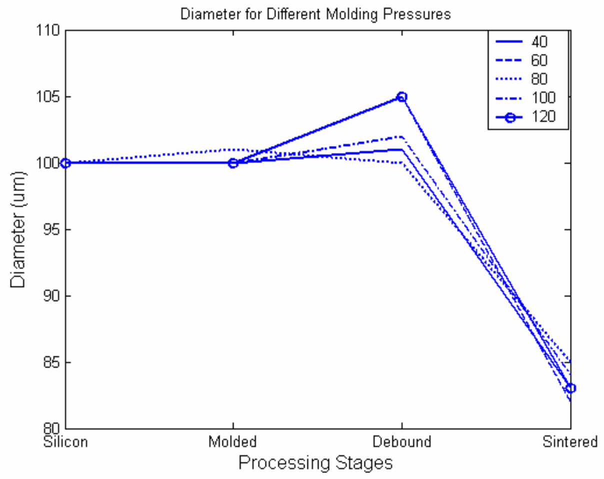

(a) Mean pillar diameter

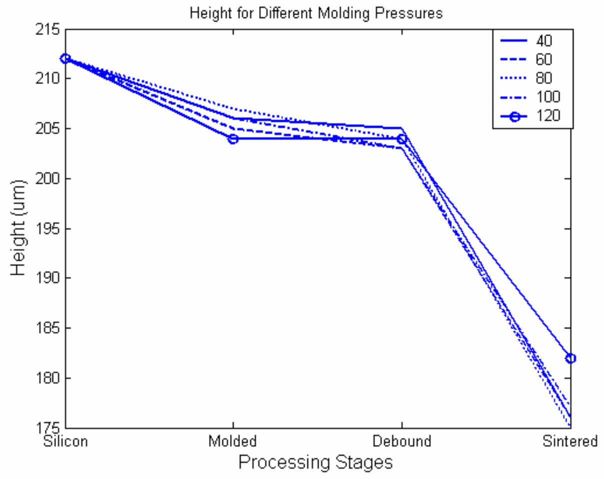

(b) Mean pillar height

Fig.11: Shrinkage by process stage for a range of molding pressures

The mechanism behind this may be the catalytic debinding method used in which the polymeric binder system is directly decomposed into gaseous components so that the inner gas pressure could result in the slight expansion. However the fact that the pillar height has tended to decrease at this stage contradicts this and indicates an overall flattening effect on the pillar shape. A further asymmetry in response is the clear decrease in pillar height compared to the Silicon master at the molded stage whilst at the same stage the diameter is unaffected. The magnitude of this effect might be expected to be linked to the molding pressure but there is no obvious correlation from these results. A further possibility is that this is due to thermal shrinkage during the cooling phase after the injection molding step. A large volumetric shrinkage of 15~20 % occurs in the sintering step and is an intrinsic feature of sintering process and is observed in both the pillar height and diameter data sets.

CONCLUSIONS

In conclusion, the dimensional variation of microstructures in the different processing steps of µMIM has been studied in this work. Parameters observed were global warpage, surface roughness and dimensional shrinkage. A pattern was observed of the warpage being consistently positive at the molded stage. There were also indications that demolding tends to flatten this curvature and that the magnitude of this effect may have some dependency on the packing pressure used in the injection molding step. After sintering there appears to be a convergence in the curvatures regardless of pressure.

Surface roughness was found to increase predictably with the removal of material in the debinding and sintering processes. There was no clear correlation between the roughness and packing pressure. Dimensional shrinkage measurements indicated that the diameter and height of the pillar structures respond differently to the process stages.

Further work will seek to relate the measured dimensional variation to material properties and further process parameters as a basis for optimization of mold insert manufacture. Additional geometric parameters such as microstructure, tilt, sidewall angle and pillar top/base concentricity may also be taken into account in future studies.

REFERENCES

[1] G. Baumeister, K. Mueller, R. Ruprecht and J. Hausselt, "Production of metallic high aspect ratio microstructures by microcasting," Microsystem Technologies, 8, 2002, 105-108.

[2] G. Fu, N. H. Loh, S. B. Tor, B. Y. Tay, Y. Murakoshi and R. Maeda, "Injection molding, debinding and sintering of 316L stainless steel microstructures," Applied Physics A: Material Science & Processing, 81, 2005, 495-500.

[3] A. Rota, T.V. Duong and T. Hartwig, "Wear resistant tools for reproduction technologies produced by micro powder metallurgy," Microsystem technologies, 7, 2002, 225-228.

[4] P. Dario, M.C. Carrozza, A. Benvenuto and A. Menciassi, "Micro-systems in biomedical applications," Journal of Micromechanics and Microengineering, 10, 2002, 235-244.

[5] C. H. Lin, G.B. Lee, B. W. Chang and G. L. Chang, " A new fabrication process for ultra-thick microfluidic structures utilizing SU-8 photoresisit," Journal of Micromechanics and Microengineering, 12, 2002, 590-597.